

# ChemComm

Chemical Communications

[rsc.li/chemcomm](http://rsc.li/chemcomm)



ISSN 1359-7345



## COMMUNICATION

Tony D. James, Nengqin Jia, Chusen Huang *et al.*  
A hemicyanine based ratiometric fluorescence probe for mapping lysosomal pH during heat stroke in living cells



Cite this: *Chem. Commun.*, 2018, 54, 5518

Received 23rd March 2018,  
Accepted 9th April 2018

DOI: 10.1039/c8cc02330a

[rsc.li/chemcomm](http://rsc.li/chemcomm)

## A hemicyanine based ratiometric fluorescence probe for mapping lysosomal pH during heat stroke in living cells<sup>†</sup>

Luling Wu,<sup>ab</sup> Yang Wang,<sup>a</sup> Tony D. James,<sup>b</sup> Nengqin Jia,<sup>b</sup>\* and Chusen Huang<sup>a</sup>\*

**Heat stroke is a lethal condition which can cause dysfunction in the central nervous system, multi-organ damage and even death. However, there is still limited knowledge of the detailed mechanism about the roles of lysosomes in heat stroke due to lack of effective tools. Herein, we introduce our previously developed hemicyanine with a large D-π-A structure as the key fluorophore to develop a new fluorescent probe (CPY) for ratiometric mapping of lysosomal pH changes in live cells under a heat shock stimulus.**

Heat stroke (HS) is a heat-related pathology when the body temperature rises to 40 °C or higher. This hyperthermia is associated with central nervous system dysfunction and dry skin, which is a life-threatening condition.<sup>1</sup> Heat stroke during annual heat waves affects immunocompromised individuals with weakened health status, as well as individuals on medications (or drug users) or certain genetic conditions, and environmental factors are also responsible for heat stroke. Additionally, long-term consequences of heat stroke increase the risk of multi-organ damage, long-term disability and even death.<sup>2–5</sup> Particularly, systemic inflammatory response syndrome is considered to be closely related to heat stroke.<sup>4</sup> However, compared to the emerging diseases that are thought to be due to heat stroke, the molecular and organelle mechanisms of this heat-related pathology are poorly understood. While, it has been found that heat shock proteins are involved in protecting heat-stroke-associated diseases,<sup>6,7</sup> information concerning heat cytotoxicity, molecular and subcellular organelle behaviour during a heat stimulus in live cells is still limited.

The lysosome is a vital subcellular organelle with a quite distinct pH (3.5–6.0) from cytoplasm (pH 7.2).<sup>8–10</sup> Due to the

appropriate acid environment, a diversity of functions such as the digestion and degradation processes of hydrolytic enzymes are maintained,<sup>11</sup> which is closely linked to other cell processes, including plasma membrane repair, energy metabolism, *etc.*<sup>12,13</sup> A steady-state lysosomal acidic environment is maintained by the proton-pumping V-type ATPase, which pumps from the cytosol to the lysosomal lumen.<sup>14–16</sup> Importantly, even a slight lysosomal pH fluctuation can have adverse effects on the cells' status. For example, abnormal lysosomal pH is associated with aging,<sup>17</sup> inflammation,<sup>18</sup> lysosomal storage diseases,<sup>19,20</sup> and tumours.<sup>20</sup> Besides physiological processes, recent studies in SW480 cells unveiled that heat stress could activate the lysosomal-mitochondrial apoptotic pathway involved in the increase of lysosomal membrane permeability.<sup>21</sup> And heat stroke might become another significant pathology responsible for aberrant lysosomal pH due to the increased lysosomal membrane permeability during a heat shock stimulus.<sup>22–24</sup> Thus, further investigation into the interplay between lysosomal behaviour and heat stroke in live cells will allow for a better understanding of the detailed mechanism of heat stroke at the subcellular level.

Examples of exploring lysosomal pH changes under a heat shock stimulus are rare despite the fact that numerous fluorescence based probes have been developed for sensing lysosomal pH in live cells.<sup>25–28</sup> To the best of our knowledge, only two examples have been previously reported for detecting lysosomal pH changes during a heat shock stimulus. Ma *et al.* used a ratiometric fluorescent probe to identify the lysosomal pH rise under heat stroke.<sup>29</sup> While Yin *et al.* developed an “off-on” naphthalimide based probe to explain the relationship between the change of lysosomal pH values and heat stroke.<sup>30</sup> However, the ratiometric fluorescent probe from Ma's group is based on the merged images of two channels to detect the pH changes in live cells and Yin's work is based on the “turn-on” fluorescence signal. Thus, a ratiometric map of lysosomal pH changes under heat stroke is still urgently needed because pH changes could then be directly observed with more accuracy and high resolution using the self-calibrated ratiometric fluorescence signal, which is of paramount importance in understanding the roles of

<sup>a</sup> The Education Ministry Key Laboratory of Resource Chemistry, Shanghai Key Laboratory of Rare Earth Functional Materials, and Shanghai Municipal Education Committee Key Laboratory of Molecular Imaging Probes and Sensors, Department of Chemistry, Shanghai Normal University, 100 Guilin Road, Shanghai 200234, China. E-mail: [nqjia@shnu.edu.cn](mailto:nqjia@shnu.edu.cn), [huangcs@shnu.edu.cn](mailto:huangcs@shnu.edu.cn)

<sup>b</sup> Department of Chemistry, University of Bath, Bath, BA2 7AY, UK.

E-mail: [t.d.james@bath.ac.uk](mailto:t.d.james@bath.ac.uk)

† Electronic supplementary information (ESI) available. See DOI: 10.1039/c8cc02330a



lysosomes in heat stroke. Herein, to develop an effective ratiometric imaging tool for mapping lysosomal pH changes in live cells under a heat shock stimulus, we designed and synthesized a new ratiometric fluorescent probe for investigating the interplay between lysosomal behaviour and heat stroke in live cells.

Our design was based on our previously developed ratiometric fluorescence based probe **CPH** that has a stable and large  $\pi$ -electron conjugated merocyanine system (D- $\pi$ -A structure), and could be used for the ratiometric fluorescence sensing of intracellular pH in live cells.<sup>31</sup> The relatively low  $pK_a$  (6.44) value of **CPH** also makes it mainly localize in lysosomes. Given that a heat shock stimulus might increase the lysosomal membrane permeability, which likely causes the leakage of the lysosomal pH indicators into the cytoplasm matrix, we attached a lysosome-targeting group, morpholine,<sup>32</sup> to **CPH** to provide a new ratiometric pH probe **CPY** (Scheme S1, ESI<sup>†</sup>) for specific labelling of lysosomes and ratiometric sensing of the lysosomal pH changes during the heat shock stimulus. Herein, the morpholine group could be used as the anchor for the localization of **CPY** in lysosomes, and the **CPH** part was taken for ratiometric sensing of pH changes (Fig. 1).

The spectroscopic properties of **CPY** were first assessed in ultrapure water with different pH values. The maximum absorption of **CPY** at 430 nm gradually shifted to 538 nm with pH values increasing from 3 to 11. And an isosbestic point was observed at 473 nm. Upon excitation at 473 nm (Fig. 3a), the maximum emission intensity at 522 nm decreased accompanied by an increase of fluorescence emission intensity at 557 nm when the pH value of the solution was increased (Fig. 3a and Scheme S1, ESI<sup>†</sup>), indicating the ratiometric fluorescence sensing of pH changes. Meanwhile, the  $pK_a$  value of **CPY** was calculated by fitting the fluorescence intensity ratio changes ( $F_{522}/F_{557}$ ) against the pH values. Interestingly, the  $pK_a$  value of **CPY** is 5.96 (Fig. S3b, ESI<sup>†</sup>), which is slightly lower than that of **CPH**. These results suggested that **CPY** could be suitable for targeting lysosomes, where the pH value is in the range of 3.5–6. We then evaluated the reversibility of the probe **CPY** using NMR analysis (Fig. S4 and S5, ESI<sup>†</sup>). The fluorescence of **CPY** in water at pH 11.0 was measured and the fluorescence intensity ratio between the maximum emission at 522 and 557 nm ( $F_{522}/F_{557}$ ) was recorded. Then the pH value of the **CPY** solution was adjusted to 3.0. The  $F_{522}/F_{557}$  ratio increased from about 0.18 to nearly 1.2 when the pH value of the water solution decreased from 11 to 3. This sensing process could be repeated at least 5 times, indicating the high reversibility of **CPY** relative to pH changes due to protonation/deprotonation of the phenol group of **CPY** (Fig. 2).

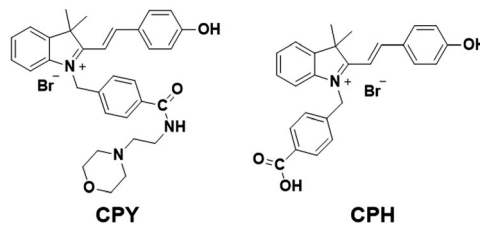


Fig. 1 Ratiometric pH probes **CPH** and **CPY**.

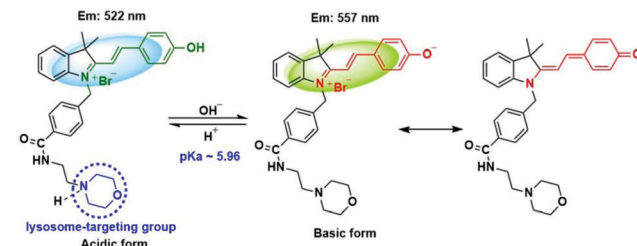


Fig. 2 pH switching of **CPY** for the ratiometric monitoring of lysosomal pH changes.

Then, the stability of the fluorescence performance of **CPY** was evaluated towards different aqueous solutions with pH values of 4.5, 7.4, and 10.5, respectively (Fig. S1b, ESI<sup>†</sup>). No change of the fluorescence ratio  $F_{522}/F_{557}$  was observed, even when the time increased to 110 min, indicating a stable pH sensing process with **CPY**. To explore if other biological reagents could interfere with the pH sensing of **CPY**, some commonly available biological species were evaluated as interferences (Fig. S1, ESI<sup>†</sup>). The ions and bioactive molecules had imperceptible influence on the fluorescence of **CPY** in both weak acid (pH = 4.5) and neutral (pH = 7.2) environments (Fig. S1c and d, ESI<sup>†</sup>). Finally, the influence of different temperatures (from 37 °C to 45 °C) on the fluorescence of **CPY** was also investigated. The fluorescence ratio  $F_{522}/F_{557}$  of **CPY** solutions at pH values of 4.0, 6.0 and 9.0, respectively, remained stable when the temperature increased from 37 °C to 45 °C. All these results demonstrated the stable fluorescence performance of **CPY** in ratiometric sensing of pH changes (Fig. S6, ESI<sup>†</sup>).

The excellent photophysical performance of **CPY** prompted us to investigate its sensing performance towards intracellular pH in live cells. CCK-8 assays were initially conducted to evaluate the cytotoxicity of **CPY**. After the cells were treated with **CPY** for 24 h, no changes in cell viability were observed when the concentration of **CPY** is below 50  $\mu$ M (Fig. S7, ESI<sup>†</sup>). However, it is interesting that some cytotoxicity for HeLa cells is observed when the concentration of **CPY** was increased to 70  $\mu$ M, which was not observed for our previously reported probe **CPH**. We deduced that this phenomenon was a result of the alkaline morpholine moiety of **CPY** which could specifically interact with lysosomes and the long incubation (24 h) will lead to an increase of lysosomal pH and induce the apoptosis of the HeLa cells. Herein, 50  $\mu$ M of **CPY** was used for the live cell imaging and no significant cytotoxicity was observed. Then, confocal laser

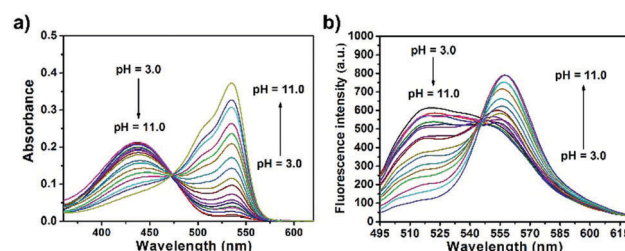


Fig. 3 (a) Absorption and (b) fluorescence response of **CPY** (10  $\mu$ M) towards different pH values in solutions containing 0.1% DMSO as a co-solvent ( $\lambda_{ex}$  = 473 nm).



scanning microscopy (CLSM) was used to perform ratiometric fluorescence imaging with **CPY** in live cells. A fluorescence signal in both channel 1 (green, 500–550 nm) and channel 2 (yellow, 570–620 nm) was observed, suggesting good cell membrane penetration of **CPY** and its potential application in intracellular labeling (Fig. S8, ESI†). In addition, the fluorescence signal from both channels was localized in a small and spherical zone, indicating lysosomal labeling. Considering the lysosomal pH range of 3.5–6.0,<sup>8</sup> the  $pK_a$  value of **CPY** (5.96) makes it localize in lysosomes and exist both in acidic and basic forms. It is notable that the relatively strong fluorescence signal from channel 1 compared to the fluorescence in channel 2 revealed that the acidic form of **CPY** is preferable to the basic form of **CPY** in the lysosomal environment (Fig. S8, ESI†).

To confirm whether **CPY** is a promising lysosome-targeting probe, colocalization experiments were conducted. The commercially available lysosome probe Lysotracker Deep Red was co-stained with **CPY** in live cells (Fig. S10a, b and S9, ESI†). The Pearson's correlation coefficient was calculated to be 0.898, which is higher than our previously reported probe **CPH** (Table S1, ESI†). These results indicated that the weakly basic amine – morpholine group – could improve the lysosome-targeting specificity. Furthermore, both the linear region of interest (ROI) and 3D surface plot analysis with the ImageJ software showed a large overlap between the **CPY** stained fluorescence signal and the commercial Lysotracker Deep Red stained signal (Fig. S10c–f, ESI†). Meanwhile, the **CPY** stained fluorescence signal collected from channel 1 also has the similar overlay results with the commercial Lysotracker Deep Red signal (Fig. S9 and S10, ESI†). All the results indicated that **CPY** was a lysosomal specific labelling probe and could be used for the ratiometric fluorescence sensing of pH changes of lysosomes in live cells.

**CPY** was then used to investigate the fluctuation of lysosomal pH during heat stroke by ratiometric fluorescence imaging. Temperatures of 41 °C and 45 °C were used as model heat stroke temperatures, while 37 °C was used as the control (normal temperature). It has been shown that temperature could induce the pH increase of lysosomes due to increased membrane permeability.<sup>29,30</sup> In order to confirm whether **CPY** could still accumulate well in lysosomes under heat stroke, colocalization experiments were conducted in live cells at 41 °C and 45 °C, respectively. Then the cells were cooled to normal temperature under incubation at 37 °C for another 20 min. The **CPY** signal collected at channel 2 (yellow) had a significant overlap with the commercial Lysotracker Deep Red signal, indicating the superior lysosome-targeting specificity of **CPY** under heat stress (Fig. 4). This phenomenon could be ascribed to the presence of the lysosome-targeting group morpholine, which was trapped in the lysosomes during the heat stress stimulus. Finally, the ratiometric sensing of pH changes in lysosomes under heat stroke was performed in live HeLa cells. Compared to the fluorescence images from the control group of HeLa cells stained with **CPY** at 37 °C for 40 minutes, the fluorescence images of **CPY** (50  $\mu$ M) loaded HeLa cells at 41 °C or 45 °C exhibited a gradual decrease in green fluorescence (channel 1, 500–550 nm) and simultaneous enhancement in the yellow fluorescence (channel 2, 570–620 nm) as the temperature increased. Moreover, the ratiometric images

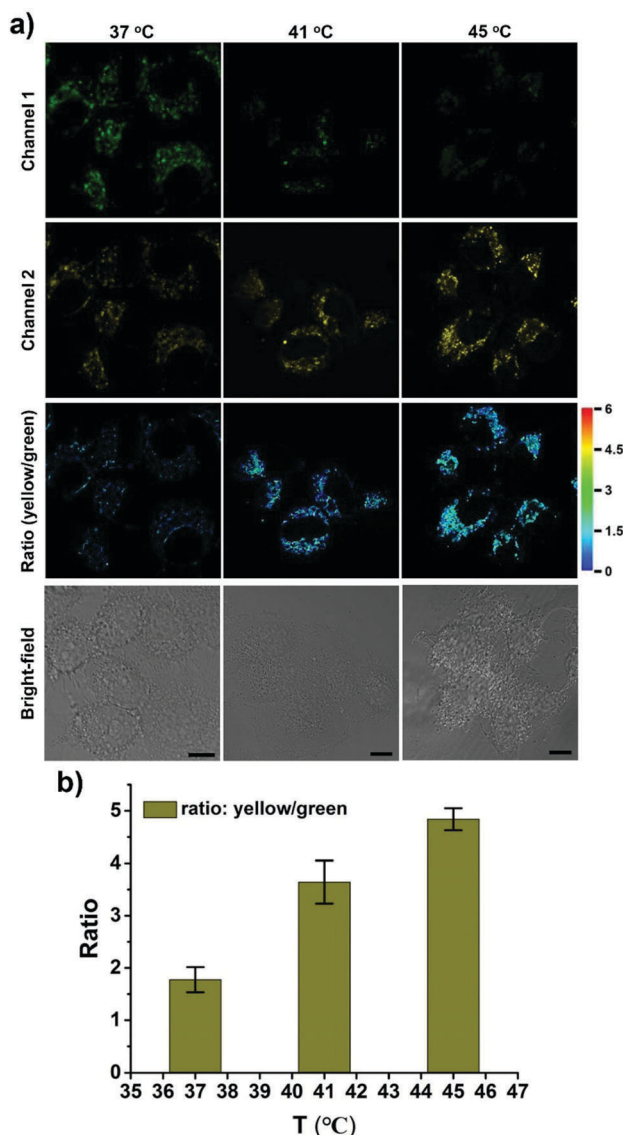


Fig. 4 Relationship between lysosomal pH changes and heat stroke in HeLa cells. (a) Ratiometric fluorescence images of the **CPY**-stained cells under heat shock at 37 °C, 41 °C, and 45 °C (left to right) respectively for 20 min and then continued culture for another 20 min at 37 °C. Excitation wavelength for **CPY**: 488 nm; emission collection, channel 1 (green, channel 1): 500–550 nm; channel 2 (yellow, channel 2): 570–620 nm. Scale bar is 10  $\mu$ m. (b) Semi-quantitative determination of **CPY**-stained HeLa cells according to the ratio of average fluorescence intensity of channel 2 (yellow) to channel 1 (green). Error bars represent s.d.

were constructed from the fluorescence signals in the yellow channel (channel 2) relative to the green channel (channel 1) using the ImageJ software (Fig. 4a, ratio (yellow/green)). After the cells were exposed to an increased temperature, the pH increase in lysosomes was clearly mapped through the ratiometric signal from the fluorescence ratiometric images. The ratiometric images taken using **CPY** stained cells could provide clearly visible information about the pH distribution in lysosomes under heat stroke. Additionally, the fluorescence emission ratio values of average emission intensity for yellow images (channel 2) and green images (channel 1) were calculated using semi-quantitative calculations (Fig. 4b).



Correspondingly, the average fluorescence emission ratio values increased from about 1.78 to 4.84 under heat stress.

Notably, all the heat shock experiments were conducted on cells that were firstly treated with heat stress at 41 and 45 °C, respectively, followed by cooling to normal temperature under incubation at 37 °C for another 20 min. Compared to the control cells that were incubated at 37 °C for another 40 min, the ratiometric fluorescence signal from the heat shock stimulus increased even when the cells were cooled to normal temperature under incubation at 37 °C for another 20 min after the heat stroke stimulus, which confirms the previous research result that the increase in lysosomal pH during heat shock is an irreversible process.<sup>29</sup>

An uneven pH distribution among lysosomes was also captured using enlarged ratiometric images (Fig. S13, ESI†), suggesting that not all lysosomes in one cell have the same response to heat stroke. Commonly several hundred lysosomes may be present in a single animal cell, which might be ascribed to the existence of different types of lysosomes with various functionalities in live cells.<sup>33,34</sup> Thus, it is an interesting phenomenon that might point to differences in individual lysosomal behavior in a single cell during heat stress.

In summary, a new ratiometric fluorescent probe (**CPY**) was synthesized for the detection of pH changes in lysosomes under heat stroke. This was achieved by introducing a lysosomal targeting group morpholine into our previously developed ratiometric pH sensitive probe **CPH**; **CPY** contains both ratiometric pH sensing ability and lysosomal localization. Our results demonstrated that **CPY** has a high selectivity and stability in the sensing of pH fluctuation through ratiometric fluorescence signal readout. Live cell imaging suggested that **CPY** was mainly trapped in lysosomes and there is little leakage even during heat stroke. More importantly, unlike the previously reported fluorescence results constructed by merging images from both red and green channels,<sup>29</sup> the ratiometric images were constructed from the **CPY** stained fluorescence signal from the yellow channel (channel 2) relative to the green channel (channel 1). The ratiometric images from the **CPY** stained cells clearly mapped the pH increase in lysosomes with increases in temperature during heat stroke and provided visible information about pH distribution in lysosomes through the discriminating pseudo-color relative to the different pH values.

Importantly, we observed an uneven pH distribution among lysosomes during heat stroke, which may indicate that not all lysosomes have the same response to a heat stimulus. In view of the compelling role of lysosomes in heat stroke<sup>22–24</sup> and the increasing evidence for the lysosomal pH increase during heat stroke,<sup>29,30</sup> our work provides an effective ratiometric imaging tool for mapping lysosomal pH changes in live cells under a heat shock stimulus as well as a potential chemical tool for unveiling the underlying mechanism of the behavior of lysosomes during heat stroke.

We thank the National Natural Science Foundation of China (Grants 21672150 and 21302125), Alexander von Humboldt Foundation (AvH), the Doctoral Fund of Ministry of Education of China (Grant No. 20133127120005), the Shanghai “Chenguang” Program (Grant 14CG42, supported by Shanghai Municipal Education Commission and Shanghai Education Development Foundation), and the Program for Changjiang Scholars and Innovative

(IRT\_16R49). LW wishes to thank China Scholarship Council and the University of Bath for supporting his PhD work in the UK. TDJ wishes to thank the Royal Society for a Wolfson Research Merit Award.

## Conflicts of interest

There are no conflicts to declare.

## Notes and references

- 1 A. Bouchama and J. P. Knochel, *N. Engl. J. Med.*, 2002, **346**, 1978–1988.
- 2 L. Argaud, T. Ferry and Q. Le, *et al.*, *Arch. Intern. Med.*, 2007, **167**, 2177–2183.
- 3 R. F. Wallace, D. Kriebel, L. Punnett, D. H. Wegman and P. J. Amoroso, *Environ. Res.*, 2007, **104**, 290–295.
- 4 L. R. Leon and A. Bouchama, *Comprehensive Physiology*, John Wiley & Sons, Inc., 2011.
- 5 R. Carter III, S. N. Cheuvront, J. O. Williams, M. A. Kolka, L. A. Stephenson, M. N. Sawka and P. J. Amoroso, *Med. Sci. Sports Exercise*, 2005, **37**, 1338–1344.
- 6 M. Jäättelä and D. Wissing, *J. Exp. Med.*, 1993, **177**, 231–236.
- 7 N. Kourtis, V. Nikoletopoulou and N. Tavernarakis, *Nature*, 2012, **490**, 213.
- 8 J. R. Casey, S. Grinstein and J. Orlowski, *Nat. Rev. Mol. Cell Biol.*, 2010, **11**, 50–61.
- 9 M. H. Lee, J. H. Han, J. H. Lee, N. Park, R. Kumar, C. Kang and J. S. Kim, *Angew. Chem., Int. Ed.*, 2013, **52**, 6206–6209.
- 10 S. Ohkuma and B. Poole, *Proc. Natl. Acad. Sci. U. S. A.*, 1978, **75**, 3327–3331.
- 11 L. Wu, X. Li, Y. Ling, C. Huang and N. Jia, *ACS Appl. Mater. Interfaces*, 2017, **9**, 28222–28232.
- 12 C. Settembre, A. Fraldi, D. L. Medina and A. Ballabio, *Nat. Rev. Mol. Cell Biol.*, 2013, **14**, 283.
- 13 C. Settembre, R. Zoncu, D. L. Medina, F. Vetrini, S. Erdin, S. Erdin, T. Huynh, M. Ferron, G. Karsenty and M. C. Vellard, *EMBO J.*, 2012, **31**, 1095–1108.
- 14 J. Tian, L. Ding, H. Ju, Y. Yang, X. Li, Z. Shen, Z. Zhu, J. S. Yu and C. J. Yang, *Angew. Chem., Int. Ed.*, 2014, **53**, 9544–9549.
- 15 J. A. Mindell, *Annu. Rev. Physiol.*, 2012, **74**, 69–86.
- 16 Y. Ishida, S. Nayak, J. A. Mindell and M. Grabe, *J. Gen. Physiol.*, 2013, **141**, 705–720.
- 17 D. J. Colacurcio and R. A. Nixon, *Ageing Res. Rev.*, 2016, **32**, 75–88.
- 18 M. Yu, X. Wu, B. Lin, J. Han, L. Yang and S. Han, *Anal. Chem.*, 2015, **87**, 6688–6695.
- 19 A. Kogot-Levin, M. Zeigler, A. Ornoy and G. Bach, *Pediatr. Res.*, 2009, **65**, 686.
- 20 B. Winchester, A. Vellodi and E. Young, *Biochem. Soc. Trans.*, 2000, **28**, 150–154.
- 21 G. Yi, L. Li, M. Luo, X. He, Z. Zou, Z. Gu and L. Su, *Oncotarget*, 2017, **8**, 40741.
- 22 C. Zhou and R. W. Byard, *J. Forensic Leg. Med.*, 2011, **18**, 6–9.
- 23 A. K. Velichko, N. V. Petrova, S. V. Razin and O. L. Kantidze, *Nucleic Acids Res.*, 2015, **43**, 6309–6320.
- 24 M. Domenech, I. Marrero-Berrios, M. Torres-Lugo and C. Rinaldi, *ACS Nano*, 2013, **7**, 5091–5101.
- 25 J.-T. Hou, W. X. Ren, K. Li, J. Seo, A. Sharma, X.-Q. Yu and J. S. Kim, *Chem. Soc. Rev.*, 2017, **46**, 2076–2090.
- 26 J. Yin, Y. Hu and J. Yoon, *Chem. Soc. Rev.*, 2015, **44**, 4619–4644.
- 27 B. Tang, F. Yu, P. Li, L. Tong, X. Duan, T. Xie and X. Wang, *J. Am. Chem. Soc.*, 2009, **131**, 3016–3023.
- 28 A.-M. Luo, Y. Shao, K.-J. Zhang, Y.-W. Wang and Y. Peng, *Chin. Chem. Lett.*, 2017, **28**, 2009–2013.
- 29 Q. Wan, S. Chen, W. Shi, L. Li and H. Ma, *Angew. Chem.*, 2014, **126**, 11096–11100.
- 30 Y. Wen, W. Zhang, T. Liu, F. Huo and C. Yin, *Anal. Chem.*, 2017, **89**, 11869–11874.
- 31 L. Wu, X. Li, C. Huang and N. Jia, *Anal. Chem.*, 2016, **88**, 8332–8338.
- 32 L. Wang, Y. Xiao, W. Tian and L. Deng, *J. Am. Chem. Soc.*, 2013, **135**, 2903–2906.
- 33 G. M. Cooper, *The Cell: A Molecular Approach*, Sunderland (MA), Sinauer Associates, 2nd edn, 2000.
- 34 C. de Duve and R. Wattiaux, *Annu. Rev. Physiol.*, 1966, **28**, 435–492.

